earth

MDPI

Article

Early Desertification Risk in Advanced Economies: Summarizing Past, Present and Future Trends in Italy

Marco Maialetti [1], Rares Halbac-Cotoara-Zamfir [2], Ioannis Vardopoulos [3] and Luca Salvati [4,*]

[1] Independent Researcher, 00195 Rome, Italy
[2] Department of Overland Communication Ways, Foundation and Cadastral Survey, Polytechnic University of Timisoara, 300224 Timisoara, Romania
[3] Foundation for Mediterranean Studies—MeDiterrate, 15452 Psychiko, Attica, Greece
[4] Department of Methods and Models for Economics, Territory and Finance (MEMOTEF), Faculty of Economics, Sapienza University of Rome, 00185 Rome, Italy
* Correspondence: luca.salvati@uniroma1.it

Abstract: Being located in the middle of Southern Europe, and thus likely representing a particularly dynamic member of Mediterranean Europe, Italy has experienced a sudden increase in early desertification risk because of multiple factors of change. Long-term research initiatives have provided relatively well-known examples of the continuous assessment of the desertification risk carried out via multiple exercises from different academic and practitioner stakeholders, frequently using the Environmentally Sensitive Area Index (ESAI). This composite index based on a large number of elementary variables and individual indicators—spanning from the climate to soil quality and from vegetation cover to land-use intensity—facilitated the comprehensive, long-term monitoring of the early desertification risk at disaggregated spatial scales, being of some relevance for policy implementation. The present study summarizes the main evidence of environmental monitoring in Italy by analyzing a relatively long time series of ESAI scores using administrative boundaries for a better representation of the biophysical and socioeconomic trends of interest for early desertification monitoring. The descriptive analysis of the ESAI scores offers a refined representation of economic spaces in the country during past (1960–2010 on a decadal basis), present (2020), and future (2030, exploring four different scenarios, S1–S4) times. Taken as a proxy of the early desertification risk in advanced economies, the ESAI scores increased over time as a result of worse climate regimes (namely, drier and warmer conditions), landscape change, and rising human pressure that exacerbated related processes, such as soil erosion, salinization, compaction, sealing, water scarcity, wildfires, and overgrazing.

Keywords: sustainable land management; zero net land degradation; sustainability metrics; environmental management; indicator dashboard; composite index; spatio-temporal analysis; regional disparities; spatial heterogeneity; Mediterranean

Citation: Maialetti, M.; Halbac-Cotoara-Zamfir, R.; Vardopoulos, I.; Salvati, L. Early Desertification Risk in Advanced Economies: Summarizing Past, Present and Future Trends in Italy. *Earth* **2024**, *5*, 690–706. https://doi.org/10.3390/earth5040036

Academic Editor: Charles Jones

Received: 10 August 2024
Revised: 16 October 2024
Accepted: 23 October 2024
Published: 26 October 2024

1. Introduction

Advanced economic systems are increasingly threatened by land degradation (LD), e.g., in America and Europe, although they are frequently considered as socioeconomic regions less prone to desertification risk because of their geographical location and/or the considerable infrastructure that brings water and improves soil via technical means [1–3]. In Europe, and especially in Southern countries—a broadly recognized and relatively well-studied hotspot of global desertification—intense LD processes have generally been associated with a complex interplay of ecological conditions and rising human pressure [4–6]. The former includes climate aridity, recurrent droughts, soil instability, and limited vegetation cover; the latter considers rising human pressure (e.g., higher population densities in ecologically fragile districts, and industrialization and tourism development, leading to overgrazing and wildfires, among others) in conditions of poorly sustainable (or largely unsustainable) land management [7–9].

To counteract the negative effects of LD, which have been proved to increase at alarming rates, the United Nations have recently introduced a strategy called ‘zero net land degradation’ in line with the Sustainable Development Goals (SDGs) of Agenda 2030. Such a strategy encourages specific actions first limiting, and then reversing the long-term trend toward LD in order to reach the objective of stopping LD by 2050 [10]. This also means not generating more negative economic impacts from LD, both directly and indirectly [11]. The permanent monitoring of LD is crucial in any policy strategy, and especially from a zero net LD perspective [12]. Implementing specific actions that counteract the economic effects of LD necessitates scientific support based on long-term assessment programs and land inventories covering a sufficiently long time interval (in order to be historically informed) and appropriate geographical coverage [13]. Considering the evident spatial heterogeneity of LD processes—documented in several empirical studies in the recently published literature—an effective permanent monitoring for policy implementation requires the exploration of relevant patterns and processes at a particularly detailed spatial scale [14]. On the one side, (qualitative and quantitative) methodologies allowing the identification of degraded areas and the estimation of spatial trends in LD are rather common and consolidated in both advanced economies and emerging countries [15]. On the other side, efforts toward permanent monitoring for policy implementation are less continuously employed, not only in emerging countries, but also in advanced economies [16].

Permanent monitoring is the base of a complete Decision Support System (DSS) used to inform land management and policy and promote the best practices to achieve reliable estimates of LD drivers (both biophysical and economic) over time and space [17]. In other words, an effective DSS for policy implementation should provide detailed information on the patterns and processes of LD that may be comparable over time and across multiple geographical and economic locations [18]. Despite the explicit and documented level of soil vulnerability and ecological sensitivity to global (and local) warming, permanent monitoring schemes in Mediterranean Europe have become relatively rare, especially in recent times [19]. A well-known and broadly applied composite index based on a composition of elementary variables and partial indicators, like the ESA (Environmentally Sensitive Area) approach, is a possible input to any DSS, assuring comparability over time and spatial reliability of the LD estimates for both biophysical assessment and economic (monetary) accounting [20].

Being developed in the context of the EU-MEDALUS research project, the Environmentally Sensitive Area Index (ESAI) scheme—to our knowledge—is likely the most applied in Southern Europe due to its simplicity in model building and to its flexibility in the use of available (and scientifically relevant) indicators [21]. Several variables and thematic indicators have been considered in the ESAI, involving the assessment of the climate, soil quality, vegetation cover, and land use and management, together with a rough quantification of human pressure based on population density and demographic dynamics [22,23]. The results of this procedure have been routinely tested (directly) and validated (indirectly) at various spatial scales—both local and regional—in Southern Europe. Multiple experimental field and case studies documented the ability of the ESAI to monitor LD conditions under vastly different ecological and socioeconomic contexts, reflecting both dynamic and peripheral locations [24].

The empirical results of any validation procedure indicate that local-scale ESAI scores can be correlated—irrespective of the background conditions—with several independent predictors of soil and landscape degradation [25]. These outcomes may document how the ESAI is a monitoring tool that is able (i) to correctly identify the areas (potentially or effectively) affected by LD and (ii) to quantify the possible impact on local systems based on an appropriate classification system ordering land on the base of a gradient of degradation from unaffected to broadly affected places [26]. This procedure has been applied in several areas with Mediterranean conditions in order to provide a detailed inspection of multiple forces assumed to trigger (or consolidate) LD processes [27].

In spite of its flexibility and applicability to vastly different socioeconomic contexts [28], the ESAI approach has been widely applied under non-Mediterranean conditions in various countries of Northern Africa and the Middle East [29], and more recently it was used for the global monitoring of LD [30]. Unfortunately, most of these applications are cross-sectional, i.e., lacking a longitudinal approach [31]. Diachronic assessments require a broad ensemble of comparable data that are not always available over sufficiently long time windows, even in advanced economies [32]. Because of the intrinsic characteristics of the ESAI, it is assumed to be a particularly appropriate component of any DSS quantifying LD intensity in advanced economies, especially in Mediterranean ecological conditions, assuring the coherent quantification of past, present, and future trends [33]. As a matter of fact, when comparable data are available, the ESAI can be estimated for distant periods in the past with the same confidence that can be realized in more recent times [34]. Additionally, the ESAI score values can be easily forecasted using simplified assumptions and methodologies and may give a coherent rationale linking the past, present, and future trends in a unique representation of LD processes in a given socio-economic context [35].

The originality and novelty of the present study thus lie in exploiting the informational potential of the ESAI in a DSS, informing zero net LD policies for European countries, especially under Mediterranean ecological conditions [36], providing an operational example of the permanent monitoring for administrative domains (both regions and smaller districts, such as provinces) in Italy. The monitoring scheme fully based on the ESAI approach covers 60 years from 1960 to 2020, with regular observations carried out every decade in order to delineate the past and present conditions in a fully compatible manner [37]. Additionally, the monitoring scheme implements a simplified module, providing short-term scenarios of LD until 2030 and considering four assumptions (from S1 to S4) based on different climate and demographic conditions [38].

2. Materials and Methods

2.1. Study Area

The degree of LD based on a composite index summarizing the information of 14 elementary variables organized in four distinct themes (climate, soil, vegetation, and land use) and generating four partial indicators (climate quality, soil quality, vegetation quality, and land-use quality) was investigated over the whole territory of Italy [30]. The country is administratively partitioned into three geographical areas (the north, the center, and the south), 20 NUTS-2 administrative regions, and more than 100 NUTS-3 provinces covering a total surface area of nearly 301,330 km^2 [21]. The provinces in Italy range from slightly more than 90 to 110 over the study period [19]. In this work, we considered the provincial boundaries referring to the 2007 administrative setting, having 110 governing units [35]. Having the original raster file to elaborate, we extracted the needed information referring to the stable administrative boundaries in order to facilitate calculations and make statistical analysis fully comparable over time [17]. Italy displays important territorial disparities in economic growth, social development, and natural resource availability and is a relevant case study to address the interaction of biophysical and socioeconomic dimensions predisposing land to degradation processes [4].

2.2. Data Sources, Elementary Variables, and Partial Indicators

GIS-based DSSs have traditionally facilitated the accurate assessment of multiple processes leading to LD [39]. The indicators selected in the present study match a number of requirements which influence the reliability of the outcome [40], including (i) the availability and regularity of time series, (ii) the quality and reliability of data sources, and (iii) the easy computing of integrated alphanumeric and cartographic data. According to the ESA framework, the variables selected refer to four knowledge dimensions: climate, soil, land cover, and human pressure (see Table 1). Climate and soil characteristics represent the most important factors affecting LD [41]. The climate characteristics were described in the ESA framework considering together (average) the annual rainfall rates, the aridity index (operationally defined as the ratio between the annual average rainfall rate and reference annual evapotranspiration), and aspect [35]. These indicators were calculated using basic information available in the National Agro-meteorological Database of the Italian Ministry of Agriculture [42]. The database relates to meteorological data collected from about 3.000 weather stations since 1951 [43]. To ensure homogeneous and complete land coverage, the database mentioned above provided spatially interpolated meteorological data via kriging (e.g., for precipitation) and co-kriging with elevation, latitude, and distance to the sea as ancillary variables (e.g., for air temperature). These geostatistical procedures were originally implemented with the aim at creating a regular grid of 544 points with daily data on temperature, precipitation, humidity, solar radiation, and wind [44]. The average annual reference evapotranspiration was calculated using a Penman–Monteith formula [45].

Table 1. The individual variables and the partial indicators (themes) composing the ESAI, together with the measurement unit and the related statistical source adopted in the present study.

Theme	Variable	Scale	Unit of Measure	Source
Soil quality	Soil texture	1:500,000	Sensitivity class	Ministry of Agriculture, European soil database
	Soil Depth	1:500,000	mm	Ministry of Agriculture, European soil database
	Available Water Capacity	1:500,000	mm	Ministry of Agriculture, European soil database
	Slope	1:25,000	%	Ministry of Environment
Climate quality	Annual mean rainfall rate	1:500,000	mm	Meteorological statistics
	Aridity index	1:500,000	mm/mm	Meteorological statistics
	Aspect	1:25,000	Angle	Ministry of Environment
Vegetation quality	Wildfire risk	1:100,000	Sensitivity class	Corine Land Cover
	Soil erosion protection	1:100,000	Sensitivity class	Corine Land Cover
	Drought resistance	1:100,000	Sensitivity class	Corine Land Cover
	Plant cover	1:100,000	Sensitivity class	Corine Land Cover
Land management quality	Population density	1:500,000	Population km^{-2}	Census of Household
	Population growth rate	1:500,000	%	Census of Household
	Land-use intensity	1:100,000	Sensitivity class	Corine Land Cover

In addition to the climate data, the soil data were obtained from (i) a soil quality map produced in the framework of the international DISMED ('mapping sensitivity to desertification') research project funded by the European Commission [46] and derived from the European soil database at a 1 km^2 pixel resolution, (ii) an Italian database of soil characteristics ('Carta nazionale della capacità idrica dei suoli agrari'), generated from geological and soilscape maps and over 18,000 soil samples [40], and (iii) ancillary information taken from thematic cartography (ecopedological and geological maps of Italy) and additional data sources, such as Digital Elevation Models and specific land-use maps with sparse soil information [47]. Variables, including soil texture, depth, slope, and the available water capacity (regarded as a proxy for additional soil structure influencing factors such as organic matter and compaction), were selected for the application of the ESA approach [48]. The soil variables were recorded as static as they change slowly or rarely over time, and due to their nature, are infrequently measured or mapped [49]. This is the case for soil quality, which was regarded as constant in the following analysis [50].

The impact of land cover changes on LD was assessed through four standard ESA variables, including wildfire risk, the capacity of vegetation to protect soils from erosion and from the negative effects of droughts, and plant cover [51]. Such indicators were obtained from the elaboration of Corine Land Cover maps referring to 1960, 1990, and 2018. A weighting score was attributed to each land-use class in order to obtain a classification of the territory based on its different levels of sensitivity related to vegetation and landscape characteristics [52].

Finally, the impact of human pressure on LD was evaluated as a result of processes such as the relocation of people along coastal areas, settlement densification around major cities, and the intensification of agricultural systems [53]. A simple proxy representing human factors is given by the population density measured at the municipal level every ten years by the National Census of Households [54]. Moreover, the demographic variation index calculated for time horizons of ten years was defined at the same geographical scale [55]. An index of agricultural intensification was obtained from the elaboration of Corine Land Cover maps (see above); a weighting score was attributed to each land-use class in order to obtain a classification of the territory based on crop intensity [56].

2.3. Deriving Scenarios for 2030

Four scenarios were prepared for the 2010–2030 horizon through a recalculation of the ESA index using two basic climate hypotheses and two basic demographic hypotheses [35]. Soil and vegetation layers were considered constant over time because of the relatively short interval considered in the forecast (ten years). All the scenarios were derived with national coverage and at the same spatial scale as that of the ESAI historical series (1960–2020). Descriptive statistics for each scenario are provided at the regional and provincial scales [57]. Provincial figures should be regarded as preliminary and representative of more general trends and should be compared with the more stable spatial trends observed (and summarized) at the regional scale [58]. The approach used for deriving scenarios follows the 'what . . . if. . .' perspective, which is well recognized in the analysis of short-term socioeconomic scenarios and particularly suited to exploit the peculiarity of the ESAI [59]. In practice, it is a matter of fixing some contextual conditions considered more probable in the projection horizon, recalculating the ESAI accordingly at the end of the projection period, and evaluating the expected deviations compared with the reference period (1960–2010) or with a most recent observation period (2020). The climate scenarios were deduced through multivariate analysis following Salvati et al. (2011) [35].

This approach, compared with other computational alternatives, has produced reference scenarios specifically aimed at calculating the ESAI, whose inputs include for the climatic dimension both rainfall and the average annual aridity index. The exploratory methodology proposed and realized by Salvati et al. (2011) [35] was therefore preferred in this study since it was proved to be consistent with the 'what . . . if' approach and capable of providing relevant inputs to the calculation of the ESAI in the near future. In summary, a representative period of the available historical series of cumulative annual precipitation and aridity index was chosen, appropriately regionalized using the regular grid mentioned above in Section 2.2. Each year of this period, represented with descriptive variables, such as cumulative month precipitation, month temperature, and the aridity index, was regarded as a statistical analysis unit on which a multivariate procedure (principal component analysis) was applied to reduce the intrinsic complexity in the data matrix [60] and obtain a cluster of statistical units (non-hierarchical clustering). In this way, all the observation years were classified into three groups with maximum homogeneity called S0, S1, and S2. Based on the analysis of the meteorological–climatic variables associated with each year, the three groups were classified accordingly.

The S0 group represents the reference period, in accordance with the long-term climatic averages (annual precipitation: 844 mm; aridity index: 1.68 on average). The S1 period represents the years with limited deviation from the climatic average, which together formed 28% of the analyzed sample (annual precipitation: 777 mm; aridity index: 1.49 on average). The S2 period represents the years with a more evident deviation from the climatic average, both in terms of precipitation and aridity regimes, and includes another 28% of the sample (annual precipitation: 716 mm; aridity index: 1.35 on average). As can be seen from the table above, the S1 scenario indicates a moderate trend toward more arid conditions with a decrease from 1.68 to 1.49 in the aridity index at the national scale, while the S2 scenario highlights more critical conditions, with an evident reduction in the aridity index and a marked decline in average annual precipitation at the national scale.

The S1 scenario, in particular, delineates the climatic averages close to what was observed for precipitation and the aridity index in the 20 years between 1991 and 2010, while the S2 scenario represents the process of further, moderate drying. Therefore, the S1 and S2 scenarios were used—together with the demographic scenarios—in the composition of the final ESAI projection according to the 'what . . . if' logic [61].

In regard to the demographic aspects, population projections take on particularly problematic aspects on the basis of recent demographic dynamics, linked not only to the intrinsic aspects of (natural) growth, but also to the increasingly significant contribution of the migratory component that is intrinsically volatile over long time horizons [62]. In this regard, the selected variables were population density, also understood as a proxy for the spatial distribution of the population and the average annual growth rate of the resident population [57]. When having to project demographic information at a spatial scale consistent with the ESAI, which is subject to strong estimation errors, it was preferred to adopt two operational scenarios in accordance with what has been achieved for the climate, analyzing the past trends from the available database and building using a digital collection (or digitalization from paper archives) of previous demographic data [58].

As for the climate, the two scenarios considered for demography represent a range of possible trends between two extremes. This rationale is, in our opinion, fully coherent with the 'what . . . if' scheme, which represents a set of possible extreme states of the system under observation. In this sense, rather than providing a point estimate (necessarily affected by a large error, given the uncertainties mentioned above), a confidence interval is provided, using two values, a base (minimum) value and a theory (extreme) value, which represent a set of possible situations within the projection time horizon [57]. For demography, the first scenario, S1, is represented by the so-called 'stable' scenario, i.e., conditions of homogeneity in time and space with respect to the last observation period (represented in this case by the observation period 2011–2020). In other words, local-scale demographic dynamics that differ from the reference average of the observation period are not excluded, but this scenario assumes that the spatial distribution of the population remains constant with respect to the reference period, for instance the demographic balance between urban and rural areas [58]. The result of these 'stable' dynamics is reflected in the (local-scale) population density consistent with the average of the observations between 2011 and 2020 and zero population growth. The second scenario, S2, instead represents a dynamic hypothesis of moderate population growth based on a longer observation period, represented by the last 20 years of observation (2001–2020). This period, particularly homogeneous with respect to the previous ones, delineates a modest population growth rate, mainly associated with changes in the migratory component, and the stabilization of the population density at high values, especially in peri-urban areas and in the most accessible rural areas, where a considerable proportion of the population resident in Italy is actually settled [3,10,42]. In this scenario, the population growth rates were assumed as equal to the ones observed at the local scale between 2001 and 2020, and the population density is derived from the sum of the population stock in 2021 and the population flow resulting from the growth processes of the period on the basis of the growth rate determined as above [62]. This scenario will lead to population density values that are possibly more impactful on the ESAI, and therefore delineates the most intense human pressure [63]. The four scenarios were determined from the recalculation of the ESAI on the basis of the inputs deriving from the intersection between the S1 (or S2) climate and S1 (or S2) demography scenarios. The possible intersections are listed as follows: Scenario S1 (S1: climate; S1: demography); Scenario S2 (S2: climate; S1: demography); Scenario S3 (S1: climate; S2: demography); and Scenario S4 (S2: climate; S2: demography). From the table above it is clear that the four proposed scenarios S1–S4 represent a range of possible projections with environmental conditions that are progressively more impactful on the ESAI. The ensemble of possible solutions between the last observation (2020) and the worst scenario represents the oscillation area of the possible variations in the ESAI in the near future.

2.4. Data Analysis

Severe LD conditions could result from a combination of inadequate land management together with a particular set of environmental factors, especially soil, climate, and vegetation [64]. The quantification of land sensitivity was carried out by evaluating the influence that each individual variable has on LD [65]. A score system was applied based on the estimated degree of correlation between the individual variables and LD. The weighting system reported in Table 2 was adopted with additional information taken from earlier studies [35,42,43,57,58].

Table 2. Indicator's weighting system by quality theme.

Soil Quality (SQI)					**Vegetation Quality (VQI)**
Texture	**Score**	**Fire Risk**	**Vegetation Type**	**Corine Class**	**Score**
S	2.00	Barren; Permanent agriculture; Crops		2.1.2., 2.2.1., 2.2.2., 2.2.3, 3.3.3, 3.3.4, 4.2.3	1.00
Si, C, SiC	1.67	Cereals; Grasslands; Deciduous forests		2.1.1., 2.4.1., 2.4.2., 2.4.3, 2.4.4., 3.1.1., 3.1.3., 3.2.1, 3.2.4	1.33
SC, SiL, SiCL	1.33	Mediterranean maquis		3.2.3	1.67
L, SCL, SL, LS, CL	1.00	Conifer		3.1.2	2.00
Soil depth		Soil erosion protection			
<15	2.00	Mixed Mediterranean maquis-evergreen wood		2.4.4., 3.1.3., 3.2.4.	1.0
15–30	1.67	Mediterranean maquis; Conifer wood; Evergreen permanent agriculture (olive trees); Permanent grassland		3.2.3., 3.1.2., 3.2.1., 3.2.3.	1.3
30–75	1.33	Deciduous wood		3.1.1.	1.6
>75	1.00	Permanent agriculture (orchard)		2.2.2.	1.8
		Crops; Grasslands; Barren		2.1.1., 2.1.2., 2.2.1., 2.4.1., 2.4.2., 2.4.3., 3.3.3., 3.3.4., 4.2.3.	2.0
Available water capacity		Drought resistance			
<80	2.00	Mixed Mediterranean maquis-evergreen wood		3.2.3., 3.2.4., 3.3.3., 3.3.4.	1.0
80–120	1.67	Conifer; Deciduous; olives		2.2.3., 3.1.1., 3.1.2., 3.1.3.	1.2
120–180	1.33	Permanent agriculture		2.2.1., 2.2.2., 2.4.4.	1.4
>180	1.00	Permanent grasslands		2.4.1., 3.2.1., 4.2.3.	1.7
Slope		Crops; Barren		2.1.1., 2.1.2., 2.4.2., 2.4.3.	2.0
>35%	2.00	Vegetation cover			
18–35%	1.67	>40%			1.0
6–18%	1.33	10–40%		2.1.1., 2.2.1., 2.2.2., 2.2.3., 2.4.1., 2.4.2., 2.4.3., 2.4.4., 3.2.1., 4.2.3.	1.8
<6%	1.00	<10%		3.3.3., 3.3.4.	2.0
Climate quality (CQI)		Land Management quality (MQI)			
Aridity index		Land-use intensity		Corine class	Score
<0.5	2.0	Olive; Deciduous and conifer wood; Mediterranean maquis		2.1.2., 2.2.1., 2.2.2., 2.4.2.	1.00
0.5–0.65	1.8	Mixed woodland-farmland areas		3.2.4., 3.3.4.	1.33
0.65–0.8	1.6	Annual crops (not irrigated); Permanent grassland		2.1.1., 2.3.1., 2.4.1., 2.4.3.	1.67
0.8–1.0	1.4	Permanent (and irrigated) agriculture		2.1.2., 2.2.1., 2.2.2., 2.4.2.	2.00
1.0–1.5	1.2	Population density			
>1.5	1.0	<100			1.0
Annual rainfall rate		100–200			1.2
<280	2.0	200–400			1.4
280–650	1.5	400–700			1.6
>650	1.0	700–1000			1.8
Aspect		>1000			2.0
−1°	1.00	Population growth rate			
225–359°	1.00	<20%			1.0
0–135°	1.00	20–40%			1.5
136–224°	2.00	>40%			2.0

Elaborating on the elementary variables mentioned above, the ESAI scheme produced four (partial) indicators—the Climate Quality Index (CQI), the Soil Quality Index (SQI), the Vegetation Quality Index (VQI), and the land Management Quality Index (MQI). These were estimated as the geometric mean of the different scores assigned to each input variable [57]. The final ESAI value was then estimated at each spatial unit (1 km^2 grid) as the geometric mean of the four partial indicators described above appropriately transformed into a score ranging from 1 (the lowest level of degradation) to 2 (the highest level of degradation) based on the system introduced by Recanatesi et al. [58]. The scoring system was extensively verified in the field, both directly and remotely [52,54]. Four partial indicators depicting environmental quality in terms of climate (Climate Quality Index, CQI), soil (Soil Quality Index, SQI), vegetation (Vegetation Quality Index, VQI), and land management (land Management Quality Index, MQI) were estimated as the geometric mean of the different scores for each variable. The ESAI was subsequently estimated in each i-th spatial unit and j-th year as the geometric mean of the four partial indicators [30] as follows:

$$ESAI_{i,j} = (SQI_{i,j} * CQI_{i,j} * VQI_{i,j} * MQI_{i,j})^{1/4}$$

The ESAI scores range from 1 (the lowest land sensitivity to desertification) to 2 (the highest sensitivity to desertification). Four classes of land sensitivity were identified based on the ESAI figures (Table 3), which reflect the most used classification thresholds [66]: (i) the areas unaffected by LD (ESAI < 1.17), (ii) the areas potentially affected (1.17 < ESAI < 1.225), (iii) the 'fragile' areas (1.225 < ESAI < 1.375), and (iv) the 'critical' areas (ESAI > 1.375). Intermediate and final maps were produced after the various elementary layers were registered and referenced to an elementary pixel of 1 km^2 [67]. Average ESAI figures were estimated for each decade, together with the percent difference over time within three geographical partitions of the Italian territory, i.e., the three main geographical sectors (the north, the center, and the south).

Table 3. The land classification system implemented with the ESAI.

ESAI Score	Class	Land Description (Examples)
<1.175	Unaffected	Areas unexposed to early desertification risk
1.175–1.225	Potentially affected	Areas potentially exposed to early desertification risk, under climate warming, depending on a particular combination of land-use or where off-site impacts will produce severe issues in surrounding territories
1.225–1.375	Fragile	Areas in which any changes in the delicate balance of natural and human activities is likely to bring about LD. For instance, the impact of predicted climate change could affect vegetation cover, intensify soil erosion, and finally shift the level of sensitivity of the area to the 'critical' class. A land-use change (e.g., a shift towards cereal cultivation on sensitive soils) might produce immediate increase in runoff and soil erosion, and perhaps pesticide and fertilizer pollution down-stream
>1.375	Critical	Areas already degraded because past land misuse, showing a threat to the environment of the surrounding land (e.g., badly eroded areas experiencing severe runoff and sediment loss).

In agreement with the National Action Plan to Combat Desertification, this partition allows for the classification of the investigated territory using different geographical and political levels that are easily interpretable for stakeholders and practitioners and support the identification of active strategies to combat early desertification and mitigate the depletion of land resources [68]. Descriptive statistics of the ESAI score were calculated for each spatial territorial unit using the 'zonal statistics' tool provided by ArcGIS software (ESRI, Inc., Redwoods, CA, USA: release 10.8.2), and we computed a weighted mean area of the score recorded on each elementary pixel and belonging to a given spatial unit [69].

3. Results

The empirical findings of this study are presented in three separate sections. Section 1 illustrates the basic, descriptive analysis of the average distribution of the ESAI scores across the three geographical regions of Italy, delineating the past, present, and future trends. Section 2 provides specific evidence on the statistical characteristics of the trends, considering the evolution of the average ESAI score and its variability over time separately for the three geographical regions and for the country as a whole. Section 3 finally delineates the results of a more specific analysis informing zero net LD strategies, which quantifies the frequency of Italian NUTS-3 provinces accomplishing the policy target (i.e., zero net increase in LD exposure over time), exploiting the ESAI statistics along four-time intervals (1960–1990, 1990–2020, 2020-S2, and 2020-S3). Scenarios S2 and S3, respectively, indicate the most and the least negative predictors of the ESAI scores for 2030.

3.1. The Latent Increase in Land Degradation Exposure of Italian Regions

An evident increase in the average ESAI scores was observed in Italy, shifting rapidly from 1.345 (1960) to 1.37 (2020), and possibly increasing even to 1.38 in the worst scenarios (S2 and S4) for 2030 (Table 4). Based on the simplified ESAI classification system (see Table 3 above), this trend underlies a shift from 'fragile' land to mostly 'critical' land, the most exposed class to LD, for Italy. Considering the three macro-regions separately (the north, the center, and the south), it can be seen how the specific level of exposure changes over time across Italy, although common trends can be envisaged similarly in all three macro-regions. The northern and central regions seem to be experiencing very similar dynamics and display average ESAI scores that are coupled over time and follow the same increase (from 1.33 to 1.36), maintaining a bit below the 'critical' threshold. The southern regions were structurally exposed to LD in 1960 (1.38). The exposure levels increased in intensity in 2020 (1.39). The scenarios were particularly critical in all the cases (between 1.40, S1 and S3, and 1.41, S2 and S4).

Table 4. Average ESAI score by geographical macro-region in Italy, 1960–2030 (scenarios S1–S4).

Region	1960	1970	1980	1990	2000	2010	2020	S1	S2	S3	S4
North	1.326	1.343	1.338	1.337	1.340	1.353	1.358	1.357	1.366	1.355	1.364
Centre	1.332	1.350	1.358	1.349	1.350	1.357	1.354	1.362	1.376	1.359	1.373
South	1.383	1.417	1.410	1.396	1.408	1.409	1.394	1.399	1.410	1.399	1.410
Italy	1.345	1.367	1.365	1.358	1.363	1.371	1.368	1.371	1.382	1.369	1.380

Figure 1 illustrates the spatial distribution of the ESAI at the beginning (1960) and the end (2020) of the study period, depicting the main spatial trends toward an increasing (or decreasing) level of land exposure to degradation over time. The maps indicate a substantial level of vulnerability to LD in specific districts of Southern Italy, with persistent and worse conditions for Sicilian and Sardinian land and extensive areas of Apulia, Basilicata, and Calabria in both 1960 and 2020. At the same time, the environmental and socioeconomic conditions at the base of the ESAI worsen during the investigated time interval in some specific areas of Northern Italy, especially the Po Valley, and along the Adriatic coastal rim, from Emilia Romagna to the north to Molise and the south. The coherent and comparative scrutiny of both maps separates the spatially persistent conditions of LD—mainly concentrated in Southern Italy—from the spatially evolving conditions predisposed to LD most frequently observed in the central and northern regions.

3.2. Profiling the Evolution over Time of the ESAI Scores in Italy

The pour plots illustrating the relationship between central tendency and dispersion over time give insights in the evolution of the LD exposure of Italian lands using descriptive statistics (Figure 2). The central tendency (mean) and dispersion (coefficient of variation) of the ESAI scores calculated as statistical aggregates of the Italian provinces by geographical region (the north, the center, and the south) delineate slightly different dynamics across the regions. In Northern Italy, the plot highlights a linear and direct relationship between the average ESAI and its standardized variability over time. When the average exposure level increases at the provincial level, the corresponding variability in the ESAI scores increases as well. This process delineates a less-predictable context at higher levels of exposure to LD because of the consequent higher volatility of the ESAI estimates at the same spatial domains. Such a relationship clearly describes the time lapse from 1960 to 2030 (considering the mean of the four scenarios, S1–S4). The central regions displayed less-linear and more-articulated dynamics, indicating a positive relationship between the average ESAI and its coefficient of variation. Conversely, the level of spatial variability in the ESAI scores decreased systematically and almost linearly over time, while maintaining high and rather stable values of the mean scores. This means that the slight increase in the level of exposure in Southern Italy is particularly homogeneous across local territories. Aggregating all the data in a unique plot for Italy as a whole, we outline a mixed trend that integrates the different conditions observed at the regional scale, and thus document the importance of regionalized approaches to LD exposure in advanced economies. The national trends were often assumed as heterogeneous phenomena reflecting mixed and largely differentiated patterns at the local scale.

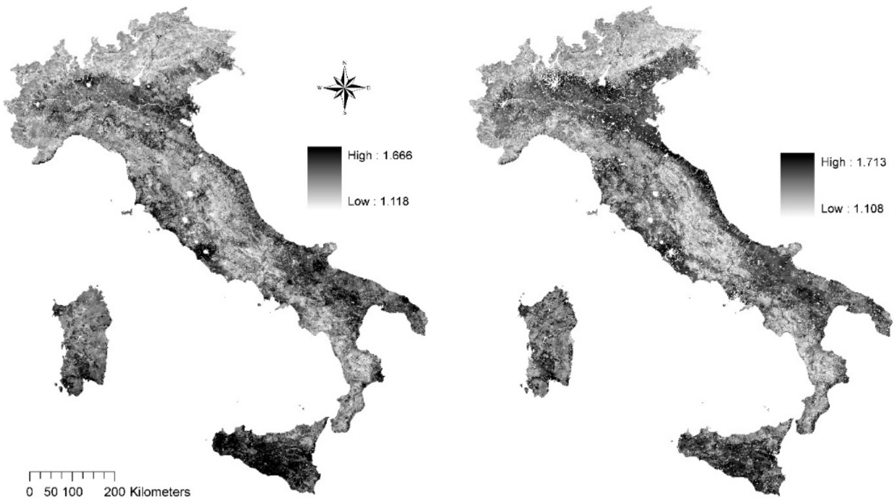

Figure 1. The spatial distribution of the ESAI scores observed all over Italy at the beginning (1960, **left**) and the end (2020, **right**) of the observation period.

3.3. Reaching Zero Net Land Degradation Targets: The Condition of Italian Provinces

Table 5 reports the percent share of the provinces reaching the target of zero net LD over the four time intervals (1960–1990, 1990–2020, 2020–2030, following the less-negative S3 scenario, and 2020–2030, following the worst S2 scenario). Thirty years were considered an appropriate time interval to empirically test such an approach. Reaching the target does not mean that specific policies were applied in the area; instead, the approach provides an expedited estimation of the percent growth rates of the ESAI score as a proxy of LD increase. The provinces with negative (or null) growth over time in the ESAI (i.e., average score decline or stability) were considered automatically compliant with the final target of this strategy. It seems clear how the first time interval indicates the northern areas as more 'compliant' with the structural target of zero net LD, i.e., four provinces out of ten experienced a negative growth rate in the ESAI score (only three and two out of ten for Southern and Central Italy). Interestingly, this trend was completely reversed in the following time interval (1990–2020), since nearly 45 provinces out of 100 were 'compliant' with a zero net target in both Central and Southern Italy, and there were only 6 in Northern Italy. While being initially associated with structurally dry and remote districts in Southern Italy (1960), it is clear how LD exposure progressively became a problem of the traditionally unaffected districts of Northern Italy (2020). The future scenarios provided less comforting news. In the case of the less-negative scenario (S3), the northern areas become mostly compliant (65 out of 100), and the reverse pattern was observed for the central and southern regions. However, in the worst scenario (S2) for 2030, only 15–20 provinces resulted in compliance with the structural target of a zero net LD strategy.

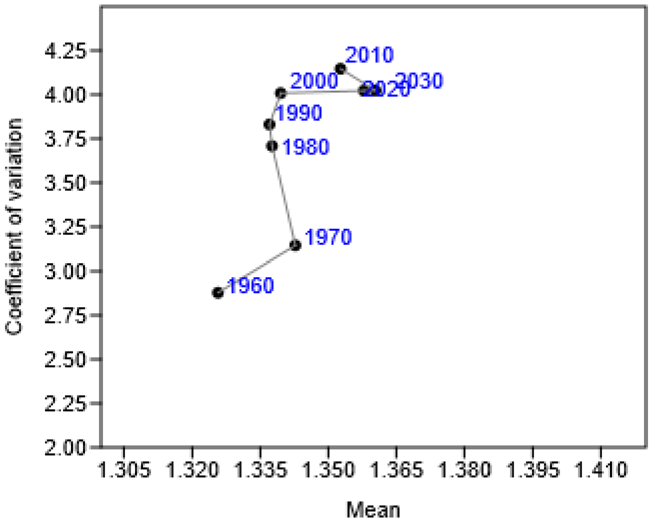

(**a**)

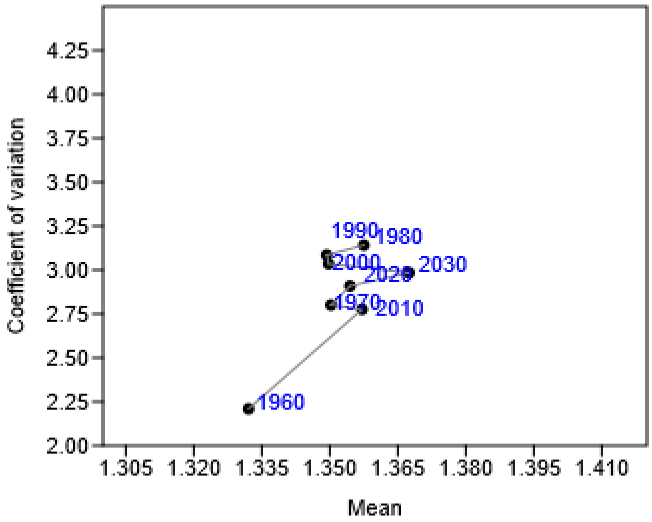

(**b**)

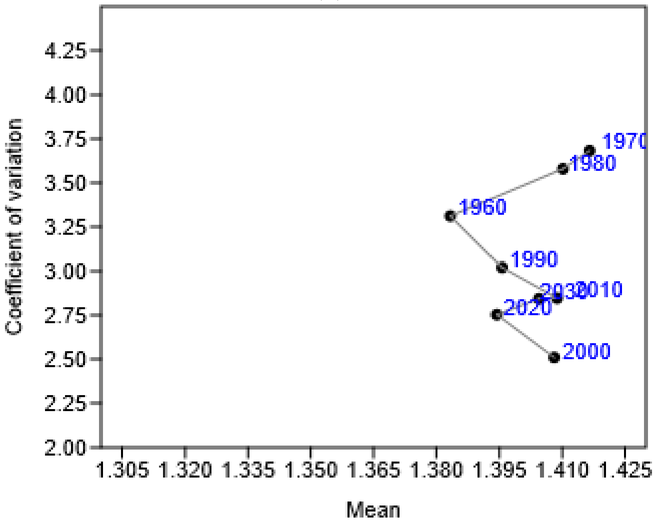

(**c**)

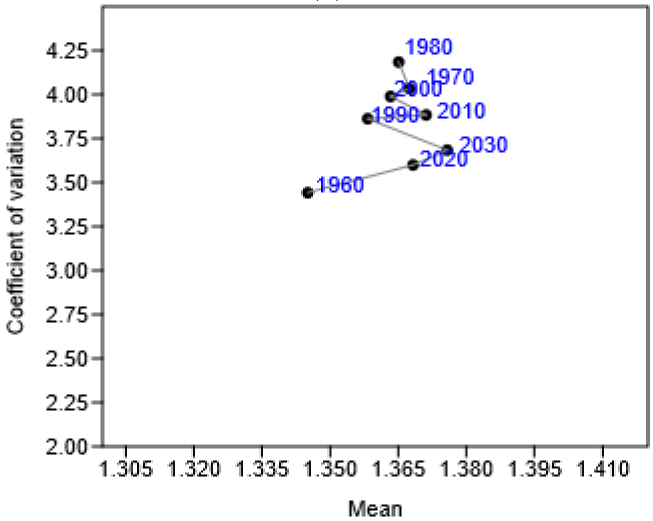

(**d**)

Figure 2. A mean-to-dispersion plot depicting the relationship over time (1960–2030) between the average ESAI score and its coefficient of variability across the Italian provinces by geographical macro-region ((**a**): Northern Italy; (**b**): Central Italy; (**c**): Southern Italy; (**d**): Italy. 2030 indicates the mean value of ESAI score and its variability across the four scenarios, from S1 to S4).

Table 5. The per cent share of provinces reaching the target of zero net LD over four time intervals (1960–1990, 1990–2020, 2020–2030, following the less negative S3 scenario, and 2020–2030, following the worst S2 scenario).

Region	60–90%	90–20%	20-S3%	20-S2%
North	41.7	6.3	64.6	14.6
Centre	17.9	46.4	28.6	14.3
South	32.4	44.1	38.2	20.6

4. Discussion

Taken as one of the most characteristic and threatening geo-hazards, LD is a global process leading to a generalized loss in soil fertility, biodiversity, ecosystem services, and landscape quality, including aesthetics. In semi-arid and dry areas, including those in advanced economies, LD—when associated with biophysical dynamics and socioeconomic factors moving toward worse predisposing conditions—has often been used to leverage the irreversible processes of soil and habitat deterioration [70]. This may lead to early desertification signs, possibly determining the reduced economic viability of soils because of sealing, compaction, contamination, salinization, and erosion, among others [71]. The inherent complexity of LD is a challenge for both science and policy [72].

Originally related to arid climates and economically disadvantaged (or peripheral) districts, a scientific consensus—based on both theoretical approaches and practical exercises—has been reached on the fact that the desertification risk has systematically grown in advanced economies all over the world [73]. The main causes of such a trend may be attributed to global (and local) warming and rising human pressure in terms of population density, industrialization, tourism growth, the expansion of services, and other high-value-added activities [5]. At the same time, within the more general strategy delineating 16 SDGs [74], the United Nations have introduced the target of zero net LD by 2050 [75]. The complex interplay of environmental and economic issues at the base of early desertification risk identification clearly encompasses political boundaries and administrative assets. Permanent monitoring is thus recommended to reach a good balance between scientific advancements and policy instruments also in light of the establishment of a continuous monitoring system of the formal (and informal) advancements toward the zero net LD targets [76].

The required (fine) tuning of science and policy will contribute to containing, mitigating, and adapting local communities and ecological systems to the future challenges of climate change, landscape transformations, and demographic modifications ultimately leading to desertification risk [77]. In this perspective, Southern Europe is a relevant example of dynamic countries exposed to early desertification risk needing the permanent monitoring of the policy targets of zero net LD [57]. Being located in the middle of Southern Europe, and thus likely representing the most dynamic economy of Mediterranean Europe, Italy has experienced a sudden increase in early desertification risk in recent decades [58]. This happened because of the joint action of multiple factors of change [30]. At the same time, Italy represents a relatively well-known example of continuous LD assessment carried out via multiple research exercises from different academic and practitioner stakeholders using the ESAI in most of these studies [52,54].

A large number of elementary variables and individual indicators, spanning from climate to soil quality and from vegetation cover to land-use intensity, facilitate the comprehensive, long-term monitoring of the early desertification risk at disaggregated spatial scales, being of some relevance for policy implementation [78]. With these considerations in mind, the present study summarizes the main evidence of environmental monitoring in Italy, analyzing a relatively long time series of ESAI scores. We adopted administrative boundaries for the better identification and comprehension of the biophysical and socioeconomic trends of interest in early desertification monitoring and policy implementation [79]. We provided a refined representation of economic spaces in the country during the past (1960–2010, with regular and homogeneous observations carried out on a decadal basis), present (2020), and future (2030, exploring four different scenarios: S1–S4) times.

Up to now, relatively few studies have been devoted to summarizing the changes in the level of early desertification risk in Mediterranean areas over sufficiently broad time intervals [80]. In this perspective, our work provides an 'early warning' assessment of the desertification risk in Italy using a mix of own data, experiments, and practical exercises, being supported by a considerable literature review. Considering together, likely for the first time in recent monitoring history, the past, present, and future dynamics of LD by adopting pixel-based scores of the standard ESAI is a particularly meaningful approach to informing any zero net LD strategy. The LD trends were estimated for each decade from 1960 to 2020 and projected for 2030. We elaborated four scenarios with different hypotheses concerning the climate, demography, and land use at the national, regional, and local observational scales jointly. A marked expansion in LD intensity was observed on average in Southern Italy (1960–1990) and more slightly in Northern Italy (1990–2020), documenting—over a sufficiently long time scale—the spatially asymmetric socioeconomic and ecological processes leading to worse conditions that may predispose land to intense degradation [81].

Based on the broad scrutiny of the recent literature for Italy, the main reasons at the base of such variegated trends are different and include (i) a reduction in rainfall in the flat districts of Northern Italy, which is, in turn, associated with enhanced pressures from high population density and farming intensification (1990–2020); as well as (ii) the consolidation of the local conditions leading to soil aridity, wildfires reducing vegetation cover, and the land abandonment of marginal districts triggering depopulation in remote, rural communities of Southern Italy (1960–1990). The joint assessment of the biophysical and socioeconomic conditions leading to LD proved to be meaningful when designing (i) more detailed studies that delineate specific LD processes at the local scale and (ii) novel measures aimed at mitigating LD with the final goal of obtaining a comprehensive policy framework against early the desertification risk in advanced economies [82–84].

5. Conclusions

Originally related to arid climates and economically disadvantaged districts, a scientific consensus has been reached on the fact that the desertification risk has systematically increased in advanced economies all over the world because of global (and local) warming and rising human pressure, both in terms of population density and in terms of industrialization, tourism growth, and the expansion of services and other high-value-added activities. At the same time, within the more general strategy delineating 16 SDGs, the United Nations have introduced a policy targeting a zero net LD objective by 2050. Because of the complex interplay of environmental and economic issues at the base of early desertification, encompassing political boundaries and administrative assets, permanent monitoring is recommended to fine-tune the scientific advancements and policy instruments related to mitigating and adapting to the future challenges of climate change, landscape transformations, and demographic modifications ultimately leading to desertification risk. From this perspective, Southern Europe is a relevant example of dynamic countries exposed to early desertification risk needing the permanent monitoring of the policy targets of zero net LD by 2050.

By incorporating the ESAI framework in a broader monitoring scheme assuring the permanent evaluation of LD, the results provided in this study document how appropriate DSSs can be considered as a sort of ‘early warning’ approach, signaling unsustainable levels of LD, which are possibly incompatible with the explicit targets of a zero net LD strategy. Taken as a proxy of early desertification risk in advanced economies, a diachronic DSS based on local-scale ESAI scores may precisely quantify the continuous increase in LD intensity over time as a result of worsening climate regimes (namely, drier and warmer conditions), landscape changes, rising human pressure, and related processes (soil erosion, salinization, compaction, sealing, water scarcity, wildfires, and overgrazing). While not focusing on specific soil processes, the ESAI appropriately quantifies the synergic effect of different forces potentially leading to LD. In other words, the ESAI assumes LD is a non-static and non-stationary process; this assumption justifies the permanent monitoring of the predisposing conditions to LD. In this perspective, the availability of longer time series of relevant variables, indicators, and composite indexes, as well as refined scenario analysis, including both short-term and medium-term horizons, are increasingly needed for any advancement of LD research in dynamic and affluent economics.

Author Contributions: Conceptualization, R.H.-C.-Z. and I.V.; methodology, M.M.; software, M.M.; validation, L.S., M.M. and I.V.; formal analysis, L.S.; investigation, R.H.-C.-Z.; resources, I.V.; data curation, I.V.; writing—original draft preparation, L.S.; writing—review and editing, M.M.; visualization, I.V.; supervision, R.H.-C.-Z.; project administration, I.V.; funding acquisition, R.H.-C.-Z. All authors have read and agreed to the published version of the manuscript.

Funding: This research received no external funding.

Institutional Review Board Statement: Not applicable.

Informed Consent Statement: Not applicable.

Data Availability Statement: Data are available upon a reasonable request to the corresponding author.

Acknowledgments: The warmest thanks go to Gianluigi Salvucci for continuous administrative and technical support.

Conflicts of Interest: The authors declare no conflicts of interest.

References

1. Akbari, M.; Alizadeh Noughani, M. Early warning systems for desertification hazard: A review of integrated system models and risk management. Model. *Earth Syst. Environ.* **2024**, *22*, 4611–4626. [CrossRef]
2. Amiraslani, F.; Dragovich, D. Combating desertification in Iran over the last 50 years: An overview of changing approaches. *J. Environ. Manag.* **2011**, *92*, 1–13. [CrossRef] [PubMed]
3. Seifollahi-Aghmiuni, S.; Kalantari, Z.; Egidi, G.; Gaburova, L.; Salvati, L. Urbanisation-Driven Land Degradation and Socioeconomic Challenges in Peri-Urban Areas: Insights from Southern Europe. *Ambio* **2022**, *51*, 1446–1458. [CrossRef] [PubMed]
4. Grilli, E.; Carvalho, S.C.; Chiti, T.; Coppola, E.; D'Ascoli, R.; La Mantia, T.; Castaldi, S. Critical range of soil organic carbon in southern Europe lands under desertification risk. *J. Environ. Manag.* **2021**, *287*, 112285. [CrossRef] [PubMed]
5. Vardopoulos, I.; D'Agata, A.; Escrivà Saneugenio, F.; Salvati, L. *Sprawl and the City: Realizing a Sustainable Mediterranean Urbanization*; Nova Science Publishers: Hauppauge, NY, USA, 2024; ISBN 9798895300060.
6. Briassoulis, H. Governing desertification in Mediterranean Europe: The challenge of environmental policy integration in multi-level governance contexts. *Land Degrad. Dev.* **2011**, *22*, 313–325. [CrossRef]
7. Bestelmeyer, B.T.; Okin, G.S.; Duniway, M.C.; Archer, S.R.; Sayre, N.F.; Williamson, J.C.; Herrick, J.E. Desertification, land use, and the transformation of global drylands. *Front. Ecol. Environ.* **2015**, *13*, 28–36. [CrossRef]
8. Becerril-Piña, R.; Mastachi-Loza, C.A.; González-Sosa, E.; Díaz-Delgado, C.; Bâ, K.M. Assessing desertification risk in the semi-arid highlands of central Mexico. *J. Arid Environ.* **2015**, *120*, 4–13. [CrossRef]
9. Prăvălie, R.; Patriche, C.; Bandoc, G. Quantification of land degradation sensitivity areas in Southern and Central Southeastern Europe. New results based on improving DISMED methodology with new climate data. *Catena* **2017**, *158*, 309–320. [CrossRef]
10. Barbero-Sierra, C.; Marques, M.J.; Ruíz-Pérez, M. The case of urban sprawl in Spain as an active and irreversible driving force for desertification. *J. Arid Environ.* **2013**, *90*, 95–102. [CrossRef]
11. Doukas, Y.E.; Salvati, L.; Vardopoulos, I. Unraveling the European Agricultural Policy Sustainable Development Trajectory. *Land* **2023**, *12*, 1749. [CrossRef]
12. Prăvălie, R. Exploring the multiple land degradation pathways across the planet. *Earth-Sci. Rev.* **2021**, *220*, 103689. [CrossRef]
13. Prăvălie, R.; Borrelli, P.; Panagos, P.; Ballabio, C.; Lugato, E.; Chappell, A.; Birsan, M.V. A unifying modelling of multiple land degradation pathways in Europe. *Nat. Commun.* **2024**, *15*, 3862. [CrossRef] [PubMed]
14. Vinci, S.; Vardopoulos, I.; Salvati, L. A Tale of a Shrinking City? Exploring the Complex Interplay of Socio-Demographic Dynamics in the Recent Development of Attica, Greece. *Cities* **2023**, *132*, 104089. [CrossRef]
15. Prăvălie, R.; Patriche, C.; Săvulescu, I.; Sîrodoev, I.; Bandoc, G.; Sfîcă, L. Spatial assessment of land sensitivity to degradation across Romania. A quantitative approach based on the modified MEDALUS methodology. *Catena* **2020**, *187*, 104407. [CrossRef]
16. Tsangaris, S.; Xepapadeas, A.; Yannacopoulos, A.N.; Salvati, L. Spatial Externalities, R&D Spillovers, and Endogenous Technological Change. *Reg. Sci. Urban Econ.* **2024**, *109*, 104055.
17. Imeson, A. *Desertification, Land Degradation and Sustainability*; Wiley: London, UK, 2012.
18. D'Agata, A.; Ciaschini, C.; Mosconi, E.M.; Rodrigo-Comino, J.; Vardopoulos, I.; Scarpitta, D.; Alhuseen, A.M.A.; Salvati, L. The Latent Shift from Monocentric to Polycentric Settlement Models. In *Urban Crisis: Social and Economic Implications for Southern Europe*; Sateriano, A., Ed.; Nova Science: Hauppauge, NY, USA, 2024; ISBN 9798891132429.
19. De Fioravante, P.; Strollo, A.; Cavalli, A.; Cimini, A.; Smiraglia, D.; Assennato, F.; Munafò, M. Ecosystem Mapping and Accounting in Italy Based on Copernicus and National Data through Integration of EAGLE and SEEA-EA Frameworks. *Land* **2023**, *12*, 286. [CrossRef]
20. Uzuner, Ç.; Dengiz, O. Desertification risk assessment in Turkey based on environmentally sensitive areas. *Ecol. Indic.* **2020**, *114*, 106295. [CrossRef]

21. Delfanti, L.; Colantoni, A.; Recanatesi, F.; Bencardino, M.; Sateriano, A.; Zambon, I.; Salvati, L. Solar plants, environmental degradation and local socioeconomic contexts: A case study in a Mediterranean country. *Environ. Impact Assess. Rev.* **2016**, *61*, 88–93. [CrossRef]
22. Karavitis, C.A.; Tsesmelis, D.E.; Oikonomou, P.D.; Kairis, O.; Kosmas, C.; Fassouli, V.; Quaranta, G. A desertification risk assessment decision support tool (DRAST). *Catena* **2020**, *187*, 104413. [CrossRef]
23. Vardopoulos, I.; Escrivà Saneugenio, F.; Sateriano, A.; Salvati, L. *Homage (and Criticism) to the Mediterranean City. Regional Sustainability and Economic Resilience*; River Publishers: New York, NY, USA, 2024; ISBN 9788770041775.
24. Akbari, M.; Memarian, H.; Neamatollahi, E.; Jafari Shalamzari, M.; Alizadeh Noughani, M.; Zakeri, D. Prioritizing policies and strategies for desertification risk management using MCDM–DPSIR approach in northeastern Iran. *Environ. Dev. Sustain.* **2021**, *23*, 2503–2523. [CrossRef]
25. Türkeş, M.; Öztaş, T.; Tercan, E.; Erpul, G.; Karagöz, A.; Dengiz, O.; Avcıoğlu, B. Desertification vulnerability and risk assessment for Turkey via an analytical hierarchy process model. *Land Degrad. Dev.* **2020**, *31*, 205–214. [CrossRef]
26. Egidi, G.; Quaranta, G.; Salvia, R.; Salvati, L.; Včeláková, R.; Cudlín, P. Urban sprawl and desertification risk: Unraveling the latent nexus in a Mediterranean country. *J. Environ. Plan. Manag.* **2021**, *65*, 441–460. [CrossRef]
27. Rutigliano, F.A.; Marzaioli, R.; Grilli, E.; Coppola, E.; Castaldi, S. Microbial, physical and chemical indicators together reveal soil health changes related to land cover types in the southern European sites under desertification risk. *Pedobiologia* **2023**, *99*, 150894. [CrossRef]
28. Egidi, G.; Salvati, L.; Vinci, S. The long way to tipperary: City size and worldwide urban population trends, 1950–2030. *Sustain. Cities Soc.* **2020**, *60*, 102148. [CrossRef]
29. Martínez-Valderrama, J.; Ibáñez, J.; Alcalá, F.J.; Martínez, S. SAT: A software for assessing the risk of desertification in Spain. *Sci. Program.* **2020**, *1*, 7563928. [CrossRef]
30. Ferrara, A.; Kosmas, C.; Salvati, L.; Padula, A.; Mancino, G.; Nolè, A. Updating the MEDALUS-ESA Framework for Worldwide Land Degradation and Desertification Assessment. *Land Degrad. Dev.* **2020**, *31*, 1593–1607. [CrossRef]
31. Carvalho, D.; Pereira, S.C.; Silva, R.; Rocha, A. Aridity and desertification in the Mediterranean under EURO-CORDEX future climate change scenarios. *Clim. Chang.* **2022**, *174*, 28. [CrossRef]
32. Grainger, A. The role of science in implementing international environmental agreements: The case of desertification. *Land Degrad. Dev.* **2009**, *20*, 410–430. [CrossRef]
33. Hammad, A.A.; Tumeizi, A. Land degradation: Socioeconomic and environmental causes and consequences in the eastern Mediterranean. *Land Degrad. Dev.* **2012**, *23*, 216–226. [CrossRef]
34. Kirkby, M. Desertification and development: Some broader contexts. *J. Arid. Environ.* **2021**, *193*, 104575. [CrossRef]
35. Salvati, L.; Venezian Scarascia, M.E.; Sabbi, A.; Zitti, M.; Perini, L. Breve excursus sul clima italiano con riferimenti al settore agricolo. *Boll. Della Soc. Geogr. Ital.* **2011**, *3*, 295–310.
36. Martínez-Valderrama, J.; Del Barrio, G.; Sanjuán, M.E.; Guirado, E.; Maestre, F.T. Desertification in Spain: A sound diagnosis without solutions and new scenarios. *Land* **2022**, *11*, 272. [CrossRef]
37. Hubacek, K.; Van Den Bergh, J.C.J.M. Changing concepts of 'land' in economic theory: From single to multi-disciplinary approaches. *Ecol. Econ.* **2006**, *56*, 5–27. [CrossRef]
38. Ibáñez, J.; Valderrama, J.M.; Puigdefábregas, J. Assessing desertification risk using system stability condition analysis. *Ecol. Model.* **2008**, *213*, 180–190. [CrossRef]
39. Kairis, O.; Karavitis, C.; Kounalaki, A.; Salvati, L.; Kosmas, C. The effect of land management practices on soil erosion and land desertification in an olive grove. *Soil Use Manag.* **2013**, *29*, 597–606. [CrossRef]
40. Kosmas, C.; Tsara, M.; Karavitis, C.A. Identification of indicators for desertification Effects of using treated municipal waste water for irrigation of olive trees in Greece. *Ann. Arid Zones* **2003**, *42*, 393–416.
41. Sterk, G.; Stoorvogel, J.J. Desertification–scientific versus political realities. *Land* **2020**, *9*, 156. [CrossRef]
42. Bajocco, S.; Ceccarelli, T.; Smiraglia, D.; Salvati, L.; Ricotta, C. Modeling the ecological niche of long-term land use changes: The role of biophysical factors. *Ecol. Indic.* **2016**, *60*, 231–236. [CrossRef]
43. Bajocco, S.; De Angelis, A.; Salvati, L. A satellite-based green index as a proxy for vegetation cover quality in a Mediterranean region. *Ecol. Indic.* **2012**, *23*, 578–587. [CrossRef]
44. Juntti, M.; Wilson, G.A. Conceptualizing desertification in Southern Europe: Stakeholder interpretations and multiple policy agendas. *Eur. Environ.* **2005**, *15*, 228–249. [CrossRef]
45. Huang, J.; Zhang, G.; Zhang, Y.; Guan, X.; Wei, Y.; Guo, R. Global desertification vulnerability to climate change and human activities. *Land Degrad. Dev.* **2020**, *31*, 1380–1391. [CrossRef]
46. Alliouche, A.; Kouba, Y. Modelling the spatiotemporal dynamics of land susceptibility to desertification in Algeria. *Catena* **2023**, *232*, 107437. [CrossRef]
47. Sgroi, F. Social agriculture is a strategy to prevent the phenomenon of abandonment in mountain areas and areas at risk of desertification. *J. Agric. Food Res.* **2022**, *10*, 100454. [CrossRef]
48. Lanfredi, M.; Egidi, G.; Bianchini, L.; Salvati, L. One size does not fit all: A tale of polycentric development and land degradation in Italy. *Ecol. Econ.* **2022**, *192*, 107256. [CrossRef]
49. Kulik, K.N.; Belyaev, A.I.; Pugacheva, A.M. The Role of Protective Afforestation in Drought and Desertification Control in Agro-Landscapes. *Arid Ecosyst.* **2023**, *13*, 1–10. [CrossRef]

50. Latorre, J.G.; García-Latorre, J.; Sanchez-Picón, A. Dealing with aridity: Socio-economic structures and environmental changes in an arid Mediterranean region. *Land Use Policy* **2001**, *18*, 53–64. [CrossRef]
51. Mihi, A.; Ghazela, R.; Wissal, D. Mapping potential desertification-prone areas in North-Eastern Algeria using logistic regression model, GIS, and remote sensing techniques. *Environ. Earth Sci.* **2022**, *81*, 385. [CrossRef]
52. Kairis, O.; Karamanos, A.; Voloudakis, D.; Kapsomenakis, J.; Aratzioglou, C.; Zerefos, C.; Kosmas, C. Identifying degraded and sensitive to desertification agricultural soils in Thessaly, Greece, under simulated future climate scenarios. *Land* **2022**, *11*, 395. [CrossRef]
53. Sun, C.; Feng, X.; Fu, B.; Ma, S. Desertification vulnerability under accelerated dryland expansion. *Land Degrad. Dev.* **2023**, *34*, 1991–2004. [CrossRef]
54. Salvia, R.; Quaranta, V.; Sateriano, A.; Quaranta, G. Land Resource Depletion, Regional Disparities, and the Claim for a Renewed 'Sustainability Thinking' under Early Desertification Conditions. *Resources* **2022**, *11*, 28. [CrossRef]
55. Perović, V.; Kadović, R.; Đurđević, V.; Pavlović, D.; Pavlović, M.; Čakmak, D.; Pavlović, P. Major drivers of land degradation risk in Western Serbia: Current trends and future scenarios. *Ecol. Indic.* **2021**, *123*, 107377. [CrossRef]
56. Gianoli, F.; Weynants, M.; Cherlet, M. Land degradation in the European Union—Where does the evidence converge? *Land Degrad. Dev.* **2023**, *34*, 2256–2275. [CrossRef]
57. Prokopová, M.; Cudlín, O.; Včeláková, R.; Lengyel, S.; Salvati, L.; Cudlín, P. Latent Drivers of Landscape Transformation in Eastern Europe: Past, Present and Future. *Sustainability* **2018**, *10*, 2918. [CrossRef]
58. D'Agata, A.; Cudlin, P.; Vardopoulos, I.; Schinaia, G.; Corona, P.; Salvati, L. Assessing the Spatial Coherence of Forest Cover Indicators from Different Data Sources: A Contribution to Sustainable Development Reporting. *Ecol. Indic.* **2024**, *158*, 111498. [CrossRef]
59. Modica, G.; Vizzari, M.; Pollino, M.; Fichera, C.R.; Zoccali, P.; Di Fazio, S. Spatio-temporal analysis of the urban–rural gradient structure: An application in a Mediterranean mountainous landscape. *Earth Syst. Dyn.* **2012**, *3*, 263–279. [CrossRef]
60. Perrin, C.; Nougarèdes, B.; Sini, L.; Branduini, P.; Salvati, L. Governance changes in peri-urban farmland protection following decentralisation: A comparison between Montpellier (France) and Rome (Italy). *Land Use Policy* **2018**, *70*, 535–546. [CrossRef]
61. Wijitkosum, S. Reducing vulnerability to desertification by using the spatial measures in a degraded area in Thailand. *Land* **2020**, *9*, 49. [CrossRef]
62. Prishchepov, A.V.; Müller, D.; Dubinin, M.; Baumann, M.; Radeloff, V.C. Determinants of agricultural land abandonment in post-Soviet European Russia. *Land Use Policy* **2013**, *30*, 873–884. [CrossRef]
63. Sidiropoulos, P.; Dalezios, N.R.; Loukas, A.; Mylopoulos, N.; Spiliotopoulos, M.; Faraslis, I.N.; Sakellariou, S. Quantitative classification of desertification severity for degraded aquifer based on remotely sensed drought assessment. *Hydrology* **2021**, *8*, 47. [CrossRef]
64. Lyu, Y.; Shi, P.; Han, G.; Liu, L.; Guo, L.; Hu, X.; Zhang, G. Desertification control practices in China. *Sustainability* **2020**, *12*, 3258. [CrossRef]
65. Masoudi, M.; Elhaeesahar, M.; Cerdà, A. Risk assessment of land degradation (RALDE) in Khuzestan Province, Iran. *Eurasian Soil Sci.* **2021**, *54*, 1228–1240. [CrossRef]
66. Ibáñez, J.; Gartzia, R.; Alcalá, F.J.; Martínez-Valderrama, J. The importance of Prevention in tackling desertification: An Approach to anticipate risks of degradation in Coastal Aquifers. *Land* **2022**, *11*, 1626. [CrossRef]
67. Ferrara, A.; Salvati, L.; Sabbi, A.; Colantoni, A. Soil Resources, Land Cover Changes and Rural Areas: Towards a Spatial Mismatch? *Sci. Total Environ.* **2014**, *478*, 116–122. [CrossRef] [PubMed]
68. Ferreira, C.S.; Seifollahi-Aghmiuni, S.; Destouni, G.; Ghajarnia, N.; Kalantari, Z. Soil degradation in the European Mediterranean region: Processes, status and consequences. *Sci. Total Environ.* **2022**, *805*, 150106. [CrossRef] [PubMed]
69. Vardopoulos, I.; Maialetti, M.; Scarpitta, D.; Salvati, L. Spatially Explicit Analysis of Landscape Structures, Urban Growth, and Economic Dynamics in Metropolitan Regions. *Urban Sci.* **2024**, *8*, 150. [CrossRef]
70. Shao, W.; Wang, Q.; Guan, Q.; Zhang, J.; Yang, X.; Liu, Z. Environmental sensitivity assessment of land desertification in the Hexi Corridor, China. *Catena* **2023**, *220*, 106728. [CrossRef]
71. Salako, G.; Adebayo, A.; Sawyerr, H.; Badmos, B.; Adio, A.; Jambo, U.M. MODIS derived vegetation and aridity indices account for spatial variation in desertification risk index in dry environment. *Int. J. Ecol. Dev.* **2021**, *36*, 46.
72. Martínez-Valderrama, J.; Guirado, E.; Maestre, F.T. Unraveling misunderstandings about desertification: The paradoxical case of the Tabernas-Sorbas Basin in Southeast Spain. *Land* **2020**, *9*, 269. [CrossRef]
73. Afzali, S.F.; Khanamani, A.; Maskooni, E.K.; Berndtsson, R. Quantitative assessment of environmental sensitivity to desertification using the modified MEDALUS model in a semiarid area. *Sustainability* **2021**, *13*, 7817. [CrossRef]
74. Vardopoulos, I.; Ioannides, S.; Georgiou, M.; Voukkali, I.; Salvati, L.; Doukas, Y.E. Shaping Sustainable Cities: A Long-Term GIS-Emanated Spatial Analysis of Settlement Growth and Planning in a Coastal Mediterranean European City. *Sustainability* **2023**, *15*, 11202. [CrossRef]
75. Fadl, M.E.; Abuzaid, A.S.; AbdelRahman, M.A.; Biswas, A. Evaluation of desertification severity in El-Farafra Oasis, Western Desert of Egypt: Application of modified MEDALUS approach using wind erosion index and factor analysis. *Land* **2021**, *11*, 54. [CrossRef]
76. Burrell, A.L.; Evans, J.P.; De Kauwe, M.G. Anthropogenic climate change has driven over 5 million km^2 of drylands towards desertification. *Nat. Commun.* **2020**, *11*, 3853. [CrossRef] [PubMed]

77. Abbas, A.; Abdul, J. Assessment of land sensitivity to desertification for Al Mussaib project using MEDALUS approach. *Casp. J. Environ. Sci.* **2022**, *20*, 177–196.
78. Berberoglu, S.; Cilek, A.; Kirkby, M.; Irvine, B.; Donmez, C. Spatial and temporal evaluation of soil erosion in Turkey under climate change scenarios using the Pan-European Soil Erosion Risk Assessment (PESERA) model. *Environ. Monit. Assess.* **2020**, *192*, 491. [CrossRef]
79. Ma, X.; Zhu, J.; Yan, W.; Zhao, C. Projections of desertification trends in Central Asia under global warming scenarios. *Sci. Total Environ.* **2021**, *781*, 146777. [CrossRef]
80. Zambon, I.; Benedetti, A.; Ferrara, C.; Salvati, L. Soil matters? A multivariate analysis of socioeconomic constraints to urban expansion in Mediterranean Europe. *Ecol. Econ.* **2018**, *146*, 173–183. [CrossRef]
81. Zasada, I.; Loibl, W.; Köstl, M.; Piorr, A. Agriculture under human influence: A spatial analysis of farming systems and land use in European rural-urban-regions. *Eur. Countrys.* **2013**, *5*, 71–88. [CrossRef]
82. Zucca, C.; Della Peruta, R.; Salvia, R.; Sommer, S.; Cherlet, M. Towards a World Desertification Atlas. Relating and selecting indicators and data sets to represent complex issues. *Ecol. Indic.* **2012**, *15*, 157–170. [CrossRef]
83. Hu, Y.; Han, Y.; Zhang, Y. Land desertification and its influencing factors in Kazakhstan. *J. Arid Environ.* **2020**, *180*, 104203. [CrossRef]
84. Rivera-Marin, D.; Dash, J.; Ogutu, B. The use of remote sensing for desertification studies: A review. *J. Arid Environ.* **2022**, *206*, 104829.